IL NUOVO CIMENTO **47 C** (2024) 7
DOI 10.1393/ncc/i2024-24007-2

COLLOQUIA: La Thuile 2023

Hunting for the second Higgs resonance at LHC

MAURIZIO CONSOLI([1]), LEONARDO COSMAI([2]) and FABRIZIO FABBRI([3])

([1]) *INFN, Sezione di Catania - I-95129 Catania, Italy*
([2]) *INFN, Sezione di Bari - I-70126 Bari, Italy*
([3]) *INFN, Sezione di Bologna - I-40127 Bologna, Italy*

received 10 October 2023

Summary. — According to perturbative calculations, the effective potential of the Standard Model should have a new minimum, well beyond the Planck scale, which is much deeper than the electroweak vacuum. Since it is not obvious that gravitational effects can become so strong to stabilize the potential, most authors have accepted the metastability scenario in a cosmological perspective. This perspective is needed to explain why the theory remains trapped into our electroweak vacuum but requires to control the properties of matter in the extreme conditions of the early Universe. As an alternative, we review the completely different idea of an effective potential which, as at the beginning of the Standard Model, is restricted to the pure Φ^4 sector but is consistent with the now existing analytical and numerical studies. In this approach, where the electroweak vacuum is the lowest energy state, beside the resonance of mass $m_h = 125$ GeV defined by the quadratic shape of the potential at its minimum, the Higgs field should exhibit a second resonance with a mass $(M_H)^{\rm theor} = 690 \pm 10$ (stat) ± 20 (sys) GeV associated with the zero-point energy which determines the potential depth. In spite of its large mass, this would couple to longitudinal W's with the same typical strength as the low-mass state at 125 GeV and represent a relatively narrow resonance of width $\Gamma_H = 30 \div 36$ GeV, mainly produced at LHC by gluon-gluon fusion. Thus it is interesting that, in the LHC data, there are various indications for a new resonance in the expected mass range with a statistical significance which is far from being negligible and could become an important new discovery by just adding two missing samples of RUN2 data.

1. – Introduction

The discovery at CERN [1, 2] of the narrow scalar resonance with mass $m_h = 125$ GeV, and the consistency of its phenomenology with the theoretical expectations for the Higgs boson, have confirmed Spontaneous Symmetry Breaking (SSB) through the Higgs field as a fundamental ingredient of particle physics. Still, there may be space for improving on the present description of symmetry breaking. This is based on a classical double-well potential with perturbative quantum corrections, say $V^{(\rm p)}(\phi)$ which exhibits a local minimum at $|\phi| = v \sim 246$ GeV and has quadratic shape fixed by $m_h^2 = (125$

GeV)^2. The point is that at large $|\phi|$ this is well approximated as $V^{(\mathrm{p})}(\phi) \sim \lambda^{(\mathrm{p})}(\phi)\phi^4$ in terms of the perturbative scalar coupling $\lambda^{(\mathrm{p})}(\phi)$ which includes the effects of the gauge and fermion fields and becomes negative beyond an instability scale $\phi_{\mathrm{inst}} \sim 10^{10}$ GeV. As a net result, beside the local electroweak vacuum where $V^{(\mathrm{p})}(v) \sim -10^8$ (GeV)^4, the true, absolute minimum of this perturbative potential is at $v_{\mathrm{true}} \sim 10^{26} \div 10^{31}$ GeV [3,4] (depending on the approximations and the exact values of the input parameters) with a much deeper potential value $V^{(\mathrm{p})}(v_{\mathrm{true}}) \sim -(10^{100} \div 10^{120})$ (GeV)^4.

While it is reassuring that the most accurate calculation [5] gives a tunneling time which is larger than the age of the Universe, still the idea of a metastable vacuum raises several questions. For instance, the new minimum is much larger than the Planck mass M_P, and the Planck scale is usually regarded as the scale where gravity becomes strong. Thus, at large $\phi \sim M_P$ should the problem be formulated in a curved space-time? In this case, does the second minimum disappear? Here, due to various uncertainties, there is no general consensus [6, 7] that gravitational physics at the Planck scale can become so strong to stabilize the electroweak vacuum. On the contrary, the vanishing value of the observed cosmological constant, on a particle physics scale, could imply that gravity remains weak [4] at all energies without introducing any threshold effect near M_P.

For this reason, one has been considering the metastability scenario in a cosmological perspective because in an infinitely old Universe even an arbitrarily small tunneling probability would be incompatible with our existence [8]. But, given the extreme conditions of the early Universe, the survival of the tiny electroweak minimum is somewhat surprising. As an example, before the discovery of the 125 GeV resonance, the authors of ref. [9] were concluding that, for 114 GeV $\leq m_h \leq$ 130 GeV and from the analysis of cosmological perturbations, either we live in a very special, and exponentially unlikely corner or new physics must exist below $\phi_{\mathrm{inst}} \sim 10^{10}$ GeV.

As an alternative, one can consider the completely different idea of a non-perturbative effective potential. Indeed, if SSB represents a *non perturbative* phenomenon, one could try to describe it non perturbatively. Since this cannot be done by retaining the full gauge and fermion structure of the theory, as at the beginning of the Standard Model, one could first concentrate on the pure Φ^4 sector but, in view of the substantial theoretical progress of last fifty years, try to describe SSB consistently with the existing theoretical and numerical studies. Then, as pointed out in refs. [10-12], one gets the idea of SSB as a weak 1st-order phase transition and the intuitive picture of the broken-symmetry phase as a condensate of real, physical quanta whose collective self-interaction represents the *primary* sector inducing SSB. The quartic coupling $\lambda(\phi)$ associated with this collective self-interaction is positive definite and exhibits a Landau pole. As such, this $\lambda(\phi)$ is quite distinct from $\lambda^{(\mathrm{p})}(\phi)$ in the sense that they could assume the same value at the Fermi scale

$$\lambda(v) = \lambda^{(\mathrm{p})}(v) = 3m_h^2/v^2 \tag{1}$$

but behave quite differently at very large ϕ. The basic prediction of this new scenario is the existence of a second resonance of the Higgs field with mass $M_H \sim 700$ GeV associated with the scale of the Zero-Point Energy (ZPE). In a 1st-order description of SSB this scale is much larger than the parameter m_h defined by the quadratic shape of the potential at the minimum. Moreover, with such a large mass $M_H \sim 700$ GeV, the ZPE of all known gauge and fermion fields would represent a small radiative correction. Thus, by restricting to a region around the Fermi scale, say a few TeV, the different

evolution of $\lambda^{(\mathrm{p})}(\phi)$ and of $\lambda(\phi)$ at asymptotically large ϕ should remain unobservable and the check is demanded to the experimental observation of the second resonance.

After resuming in sect. 2 this different picture of SSB, we will review in sect. 3 the basic phenomenology of the second resonance. We will then summarize in sect. 4 some recent analyses [13-16] of LHC data which, indeed, support the existence of a new resonance in the expected mass range with a non-negligible statistical evidence that could become an important new discovery by just adding two crucial, missing samples of RUN2 data. Section 5 will finally contain a summary together with some remarks about the present agreement between the Higgs mass parameter extracted indirectly from radiative corrections and the value $m_h = 125$ GeV directly measured at LHC.

2. – SSB in a Φ^4 theory

2˙1. *Preliminaries.* – Let us start from scratch with the type of scalar potential reported in the review of the Particle Data Group (PDG) [17]

$$V_{\mathrm{PDG}}(\phi) = -\frac{1}{2} m^2_{\mathrm{PDG}} \phi^2 + \frac{1}{4!} \lambda_{\mathrm{PDG}} \phi^4 \tag{2}$$

By fixing $m_{\mathrm{PDG}} \sim 88.8$ GeV and $\lambda_{\mathrm{PDG}} \sim 0.78$, this has a minimum at $|\phi| = v \sim 246$ GeV and a second derivative $V''_{\mathrm{PDG}}(v) \equiv m_h^2 = (125\ \mathrm{GeV})^2$ (one is adopting here the identification $m_h^2 = V''_{\mathrm{PDG}}(v) = |G^{-1}(p=0)|$ in terms of the inverse, zero-momentum propagator).

With eq. (2), one is assuming a double-well potential with suitably chosen mass and coupling. The instability of the symmetric vacuum at $\phi = 0$ is then traced back to the condition $V''_{\mathrm{PDG}}(\phi = 0) = -m^2_{\mathrm{PDG}} < 0$ which characterizes SSB as a 2nd-order phase transition. This traditional idea of a "tachyonic" mass term at $\phi = 0$, however, is not the only possible explanation. As in the original Coleman and Weinberg analysis [18], SSB could originate from ZPE in the classically scale invariant limit $V''_{\mathrm{eff}}(\phi = 0) \to 0^+$. In this case, if the quanta of the symmetric phase have a tiny physical mass $m^2_\Phi \equiv V''_{\mathrm{eff}}(\phi = 0) > 0$ which is below some critical value m_c^2, the symmetric phase could be "locally" stable but become "globally" unstable. By lowering the mass below m_c^2, the absolute minimum of the effective potential would then discontinuously jump from $\phi = 0$ to $\phi \neq 0$ and SSB would represent a 1st-order phase transition.

We emphasize that this idea of SSB as a weak 1st-order phase transition in Φ^4 theories finds support in lattice simulations [19-21]. To this end, one can just look at fig. 7 of ref. [21] where the data for the average field at the critical temperature show the characteristic 1st-order jump and not the smooth 2nd-order trend. This agreement with lattice simulations is a good motivation to further explore the implications of a 1st-order scenario ([1]).

([1]) We observe that conflicting indications have more recently been reported in ref. [22]. These authors, object to the traditional view that the Ising model and the Φ^4 theory (at finite bare coupling) belong to the same universality class. Thus a second-order phase transition, as in standard RG-improved perturbation theory, would not be ruled out. Still, the Ising limit, with a lattice coupling at the Landau pole, is known to saturate the triviality bound in Φ^4. Namely, at any fixed non-zero value of the renormalized coupling, it represents the best approximation to the continuum limit [23], a remark which is certainly relevant for lattice simulations of a quantum field theory. Furthermore, as discussed in Subsection 2.3, the weak first-order scenario

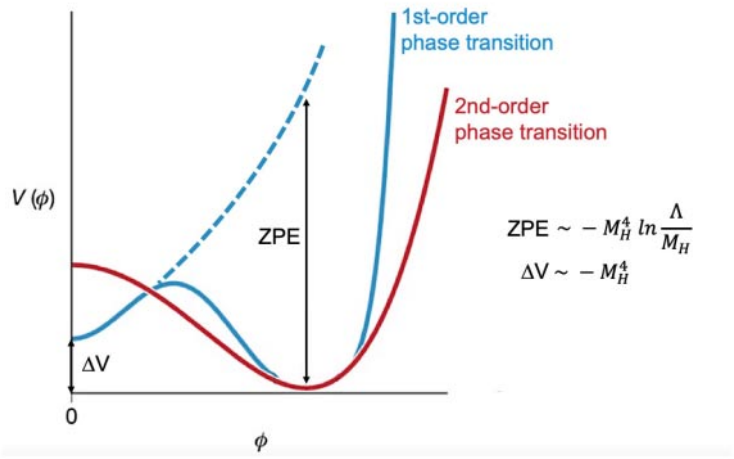

Fig. 1. – *An intuitive picture which illustrates the crucial role of the ZPE in a 1st-order scenario of SSB. Differently from the standard 2nd-order picture, these have to compensate for a tree-level potential with no non-trivial minimum.*

From a physical point of view, the motivation for a tachyonic mass term at $\phi = 0$ reflects the prejudice that Φ^4 is a pure repulsive interaction. In this case, in fact, any state made of physical massive particles would necessarily have an energy density which is higher than the trivial empty vacuum at $\phi = 0$. However, as discussed in [24], the Φ^4 interaction is *not* always repulsive. The inter-particle potential between the basic quanta of the symmetric phase, beside the $+\lambda\delta^3(\mathbf{r})$ tree-level repulsion, contains a $-\lambda^2 \frac{e^{-2m_\Phi r}}{r^3}$ attraction which originates from the *ultraviolet-finite* part of the 1-loop diagrams and whose range becomes longer and longer in the $m_\Phi \to 0$ limit ([2]). Due to the qualitative difference of the two effects, to consistently include higher order effects, one should re-arrange the perturbative expansion by renormalizing symmetrically *both* the contact repulsion and the long-range attraction as discussed by Stevenson [27]. In this way, by taking into account both effects, a calculation of the energy density indicates that, for positive and small enough m_Φ, the attractive tail dominates. Then, the lowest-energy state is not the trivial, empty vacuum with $\phi = 0$ but a state with $\phi \neq 0$ and a Bose condensate of symmetric-phase quanta in the $\mathbf{k} = 0$ mode ([3]).

2˙2. *"Triviality" and the effective potential.* – In spite of these interesting aspects, one could still wonder about different observable consequences. After all, the phenomenology of the broken-symmetry phase should only depend on the potential near the true minimum (and not at $\phi = 0$) and, in principle, nothing prevents it locally from having exactly the same shape as in eq. (2). To get insight, let us look at fig. 1. This intuitively illus-

---

of SSB in Φ^4 finds *additional* motivations when considering the class of approximations to the effective potential which are consistent with the basic "triviality" of the theory.

([2]) Starting from the scattering matrix element $\mathcal{M}$, obtained from Feynman diagrams, one can construct an inter-particle potential that is is basically the 3-dimensional Fourier transform of $\mathcal{M}$, see refs. [25, 26].

([3]) This 1st-order scenario is implicit in 't Hooft's description of SSB [28] :"What we experience as empty space is nothing but the configuration of the Higgs field that has the lowest possible energy. If we move from field jargon to particle jargon, this means that empty space is actually filled with Higgs particles. They have Bose condensed".This clearly refers to real, physical quanta. Otherwise, in a 2nd-order picture, Bose condensation of what?

trates that, if $V''_{\rm eff}(\phi=0)>0$, ZPE are expected to be much larger than in a 2nd-order picture. In the latter case, in fact, SSB is driven by the negative mass squared at $\phi=0$ while now ZPE have to overwhelm a tree-level potential which otherwise would have no non-trivial minimum. But what do we exactly mean by saying that ZPE have to be *much larger*? The answer is that, now, the ZPE mass scale M_H is much larger than the mass scale m_h defined by the quadratic shape of the effective potential at the minimum. To fully understand this crucial issue let us first recall that this large size of ZPE induced Coleman and Weinberg to expect that the weak, 1st-order scenario could only work in the presence of gauge bosons. In a pure Φ^4 theory SSB would require to compensate the positive $\lambda\phi^4$ tree-level potential with a negative $\lambda^2\phi^4\ln(\phi^2/\Lambda^2)$ 1-loop contribution; a requirement which lies outside a standard loop-expansion perspective. Instead, they concluded, with gauge bosons the corresponding 1-loop contribution $g^4_{\rm gauge}\phi^4\ln(\phi^2/\Lambda^2)$ could well represent the needed driving mechanism if $\lambda\sim g^4_{\rm gauge}$.

Nevertheless, there is a way to rearrange things in the effective potential and consistently describe SSB as 1st-order transition. The standard perspective, which is behind the idea of the perturbative potential $V^{(\rm p)}(\phi)\sim\lambda^{(\rm p)}(\phi)\phi^4$, considers the 1-loop contribution as simply renormalizing the coupling λ in the classical potential

$$\frac{\lambda}{4!}\phi^4\to\frac{\lambda}{4!}\phi^4(1-\frac{3\lambda}{32\pi^2}\ln(2\Lambda^2\sqrt{e}/\lambda\phi^2) \tag{3}$$

Therefore, including the higher-order leading logarithmic terms, *i.e.*, by replacing

$$1-x\to 1-x+x^2-x^3...=1/(1+x) \tag{4}$$

the 1-loop minimum would disappear.

But, as emphasized by Stevenson [27], the qualitatively different nature of the two basic terms in the inter-particle potential between the quanta of the symmetric phase has a definite counterpart in the structure of the effective potential. Here, the positive $\lambda\phi^4$ background originates from the $+\lambda\delta^3(\mathbf{r})$ short-range repulsion and the negative ZPE from the long-range $-\frac{\lambda^2}{r^3}$ attraction. This observation suggests to consider the equivalent reading of the 1-loop potential as the sum of a classical background + zero-point energy of free-field fluctuations with mass squared $M^2(\phi)=\lambda\phi^2/2$

$$V_{1-\rm loop}(\phi)=\frac{\lambda\phi^4}{4!}-\frac{M^4(\phi)}{64\pi^2}\ln\frac{\Lambda^2\sqrt{e}}{M^2(\phi)} \tag{5}$$

Since this type of structure is also recovered in higher-order approximations, the simple 1-loop potential can also admit a non-perturbative interpretation as the *prototype* of a class of calculations with the same basic structure up to a redefinition of both classical background and mass parameter $M(\phi)$.

This is explicitly illustrated by the Gaussian effective potential [29] which re-sums all one-loop bubbles and preserves the same structure up to terms that vanish when $\Lambda\to\infty$:

$$\lambda\to\lambda_G(\phi)=\frac{\lambda}{1+\frac{\lambda}{16\pi^2}\ln\frac{\Lambda}{M_G(\phi)}} \tag{6}$$

$$M^2(\phi)\to M^2_G(\phi)=\frac{\lambda_G(\phi)\phi^2}{2} \tag{7}$$

$$V_{1-\text{loop}}(\phi) \to V_G(\phi) = \frac{\lambda_G(\phi)\phi^4}{4!} - \frac{M_G^4(\phi)}{64\pi^2} \ln \frac{\Lambda^2\sqrt{e}}{M_G^2(\phi)} \tag{8}$$

The agreement between 1-loop and Gaussian effective potential has to be emphasized because it gives further insight into the "triviality" of Φ^4. If, in the continuum limit, all interaction effects have to be effectively reabsorbed into the first two moments of a Gaussian distribution, meaningful approximations to the effective potential should be physically equivalent to the 1-loop result, *i.e.*, given again by some classical background + zero-point energy with some $\phi-$dependent mass.

For this reason, the two approximations considered above produce similar results. Namely, by defining m_h^2 as the second derivative of $V_{1-\text{loop}}(\phi)$ or of $V_G(\phi)$ at their minimum, say $\phi = \pm\phi_v$, and by defining M_H as the value of $M(\phi_v)$ or $M_G(\phi_v)$, one finds $M_H \sim \Lambda \exp(-1/\lambda)$ and the same pattern of scales [10-12] in terms of $L = \ln(\Lambda/M_H)$ and of a cutoff-independent vacuum field v:

$$\lambda \sim L^{-1} \qquad\qquad m_h^2 \sim v^2 \cdot L^{-1} \qquad\qquad M_H^2 \sim L \cdot m_h^2 = K^2 v^2 \tag{9}$$

Here K is a cutoff-independent constant and v is related to ϕ_v through a re-scaling given by the mass ratio, namely

$$\phi_v^2 \equiv Z_\phi v^2 \qquad\qquad \text{with} \qquad\qquad Z_\phi = (M_H/m_h)^2 \sim L \tag{10}$$

Since the vacuum energy $V_{\text{eff}}(\phi_v) = -M_H^4/(128\pi^2)$ is a Renormalization-Group invariant quantity [10-12], M_H and v emerge as the two invariants $I_1 = M_H$ and $I_2 = v$ associated with the analysis of the effective potential in the (λ, ϕ, Λ) 3-dimensional space. For this reason, v represents the natural candidate to represent the weak scale $v \sim 246$ GeV. Note that in perturbation theory within the standard 2nd-order scenario, where $m_h \sim M_H$, there is no $v-\phi_v$ distinction. Instead, here, it is a consequence of minimizing the effective potential where the large logarithm $L = \ln(\Lambda/M_H)$ is effectively transformed into a $1/\lambda$ effect with strong cancelations between formally higher-order and tree-level terms. Yet, the implications of this two-mass structure may not be entirely clear. These will be illustrated in the following two subsections.

2˙3. *The coexistence of m_h and M_H.* – To further sharpen the meaning of m_h and M_H, let us recall that the ZPE is (one-half of) the trace of the logarithm of the inverse propagator $G^{-1}(p) = (p^2 - \Pi(p))$. Therefore, in a free-field theory where $V_{\text{free}}(\phi) = \frac{1}{2}m^2\phi^2$ and $|\Pi(p)| = |\Pi(p=0)| \equiv m^2$, after subtracting constant terms and quadratic divergences (or using D-dimensional regularization with the identification $\ln\Lambda \equiv 1/(4\text{-D})$ $-1/2(\gamma - \ln(4\pi))$ one finds

$$(\text{ZPE})^{\text{free}} = \frac{1}{2}\int \frac{d^4p}{(2\pi)^4} \ln(p^2+m^2) = -\frac{m^4}{64\pi^2}(\ln\frac{\Lambda^2}{m^2} + \frac{1}{2}) \tag{11}$$

Instead, in the presence of interactions, where in general $\Pi(p) \neq \Pi(p=0)$, things are not so simple. On the one hand, the derivatives of the effective potential produce (minus) the n-point functions at zero external momentum so that, by defining ϕ_v the minimum of $V_{\text{eff}}(\phi)$, one gets

$$m_h^2 \equiv V''_{\text{eff}}(\phi_v) = |\Pi(p=0)| = |G^{-1}(p=0)| \tag{12}$$

On the other hand, ZPE contribute to the effective potential but are not a pure zero-momentum quantity. Therefore, at the minimum, one can write

$$\text{ZPE} \sim -\frac{1}{4}\int_{p_{\min}}^{p_{\max}} \frac{d^4p}{(2\pi)^4}\frac{\Pi^2(p)}{p^4} \sim -\frac{\langle\Pi^2(p)\rangle}{64\pi^2}\ln\frac{p^2_{\max}}{p^2_{\min}} \sim -\frac{M_H^4}{64\pi^2}\ln\frac{\Lambda^2}{M_H^2} \tag{13}$$

This shows that M_H^2, effectively including the contribution of the higher momenta, reflects a typical average value $|\langle\Pi(p)\rangle|$ at non-zero p. In perturbation theory, where $\Pi(p) \sim \Pi(p=0)$ up to small corrections, one finds $M_H \sim m_h$. On the other hand, if $M_H \gg m_h$ *there must be* a non-trivial difference between $p=0$ and $p\neq 0$ with deviations from a standard one-mass propagator.

2˙4. *Lattice simulation of the propagator and the value of* M_H. – The existence of deviations from a standard single-particle propagator in the cutoff theory was checked with a lattice simulation [10] to extract m_h from the $p\to 0$ limit of $G(p)$ and to compare it with the mass M_H obtained from its behaviour at higher p^2. To this end, the propagator data were first fitted to the 2-parameter form

$$G_{\text{fit}}(p) = \frac{Z_{\text{prop}}}{\hat{p}^2 + m^2_{\text{latt}}} \tag{14}$$

in terms of the squared lattice momentum $\hat{p}^2$. The data were then re-scaled by $(\hat{p}^2+m^2_{\text{latt}})$ so that deviations from a flat plateau are immediately visible. While in the symmetric phase no momentum dependence of the mass parameter was observed, in the broken-symmetry phase there is a transition between two regimes. As pointed out by Stevenson [30], by rescaling all data with the mass from the higher-momentum fit, the deviations from constancy become highly significant in the $p\to 0$ limit.

In ref. [10] this was checked on a large 76^4 lattice where, to obtain a good description of the propagator data in the full momentum region, one had to use a two-mass form [12]

$$G(p) \sim \frac{1-I(p)}{2}\frac{1}{p^2+m_h^2} + \frac{1+I(p)}{2}\frac{1}{p^2+M_H^2} \tag{15}$$

with an interpolating function $I(p)$ which depends on an intermediate momentum scale p_0 and tends to $+1$ for large $p^2 \gg p_0^2$ and to -1 when $p^2\to 0$. Crucially, extrapolation toward the continuum limit with various lattices was consistent with the expected scaling trend $M_H^2 \sim Lm_h^2$ from Eqs.(9). To this end from the lattice data for the propagator one extracted a numerical constant c_2 which determines the logarithmic slope

$$\frac{M_H^2}{m_h^2}\Big|_{\text{latt}} \sim L\cdot(c_2)^{-1} \tag{16}$$

The values of $(c_2)^{-1/2} = M_H\cdot(m_h)^{-1}\cdot L^{-1/2}$ are reported in table I and, given their consistency, lead to a final determination

$$(c_2)^{-1/2} = 0.67 \pm 0.01\ (\text{stat}) \pm 0.02\ (\text{sys}) \tag{17}$$

Therefore, to estimate M_H, one adopted the following strategy:

TABLE I. – *For various values of the hopping parameter κ of the 4D Ising model, we report the mass M_H obtained from the higher-momentum propagator data by various authors and the zero-momentum m_h, see* [10]. *For $\kappa = 0.0749$ the three values of M_H refer to high-momentum fits for $\hat{p}^2 > 0.1$, $\hat{p}^2 > 0.15$ and $\hat{p}^2 > 0.2$ respectively on the 76^4 lattice of ref.* [10]. *The lattice cutoff $\Lambda_L \sim \pi/a$ and all masses are in units of the inverse lattice spacing a. In the last column, we report the combination $(c_2)^{-1/2} = M_H \cdot (m_h)^{-1} \cdot L^{-1/2}$. The table is adapted from the original table of ref.* [10].

κ	M_H	$(m_h)^{-1}$	$[\ln(\Lambda_L/M_H)]^{-1/2}$	$(c_2)^{-1/2}$
0.07512	0.2062(41)	5.386(23)	0.606(2)	0.673(14)
0.0751	~ 0.200	5.568(16)	~ 0.603	~ 0.671
0.07504	0.1723(34)	6.636(32)	0.587(2)	0.671(14)
0.0749	0.0933(28)	13.00(14)	0.533(2)	0.647(22)
0.0749	0.096(4)	13.00(14)	0.535(3)	0.668(31)
0.0749	0.100(6)	13.00(14)	0.538(4)	0.699(48)

i) first, one used the Gaussian approximation relation (valid in the whole range of m_Φ and not just for $m_\Phi = 0$)

$$M_H^2 = \frac{\lambda}{3}\,\phi_v^2 \tag{18}$$

ii) second, the re-scaling $Z_\phi = \frac{\phi_v^2}{v^2} = \frac{M_H^2}{m_h^2}$ was extracted from the lattice data for the propagator yielding

$$\frac{\phi_v^2}{v^2} = Z_\phi \sim L \cdot (c_2)^{-1} \tag{19}$$

iii) finally, in eq. (18) one used the leading-log relation

$$\lambda \sim (16\pi^2/3) \cdot L^{-1} \tag{20}$$

In this way, the constant K was determined as

$$K = (4\pi/3) \cdot (c_2)^{-1/2} = 2.80 \pm 0.04\ (\text{stat}) \pm 0.08\ (\text{sys}) \tag{21}$$

(or $K \sim 8\pi/9$) so that for $v \sim 246$ GeV one finds

$$(M_H)^{\text{Theor}} = Kv = 690 \pm 10\ (\text{stat}) \pm 20\ (\text{sys})\ \text{GeV} \tag{22}$$

The above numerical estimate, on the one hand, represents a definite prediction to compare with experiments. On the other hand, it helps to clarify the relation with the more conventional picture of a cutoff theory with only m_h. To this end, we note that, from relations (9), one finds $m_h \ll M_H$ for very large Λ. But M_H is $\Lambda-$independent so

that by decreasing Λ also the lower mass increases by approaching its maximun value $(m_h)^{\max} \sim M_H$ when the cutoff Λ is a few times M_H. Therefore this maximum value corresponds to

$$(m_h)^{\max} \sim (M_H)^{\text{Theor}} = 690 \pm 10 \text{ (stat)} \pm 20 \text{ (sys) GeV} \tag{23}$$

in good agreement with the old theoretical upper bound $(m_h)^{\max} = 670$ (80) GeV, see Lang's complete review [31]. However, in the real world $m_h = 125$ GeV so that, if there is a second resonance with $M_H \sim 700$ GeV, Λ would be extremely large.

3. – Basic phenomenology of the second resonance

The analysis of sect. 2 represents a consistent description of SSB in a Φ^4 theory. At the same time, given the large value $M_H \sim 700$ GeV, including the ZPE of all known gauge and fermion fields at the Fermi scale would represent a small radiative correction ([4]). As in the early days of the Standard Model, one could thus adopt the perspective of explaining SSB within the pure scalar sector and restrict the analysis to a region around the Fermi scale which is not much larger than a few TeV. Then, once the perturbative $\lambda^{(\text{p})}(v)$ and the scalar coupling $\lambda(v)$ responsible for SSB have the same value as in eq. (1), their different evolution at extremely large energies should remain unobservable. Checking our proposed mechanism for SSB is then demanded to the observation of the second resonance and of its phenomenology.

As for the relevant phenomenology, a Higgs resonance with mass $M_H \sim 700$ GeV is usually believed to be a broad resonance due to strong interactions in the scalar sectors. This belief derives from two arguments, namely the definition of M_H from the quadratic shape of the potential, which is not valid in our case, and the tree-level calculation of longitudinal WW scattering where, at high energy, due to an incomplete cancelation of graphs, the mass in the scalar propagator is effectively promoted to coupling constant. For sake of clarity we will consider the second argument in a high-energy regime where the Higgs field propagator is dominated by the second resonance, as in the standard one-pole calculations. From the tree-level expression reported by Veltman and Yndurain [32] we then get

$$A_{\text{ww}} = \frac{g^2}{4M_w^2} \left[a_{\text{tree}}(s) + a_{\text{tree}}(t) + a_{\text{tree}}(u)\right] \tag{24}$$

where $g = g_{\text{gauge}}$, $M_w^2 = g^2 v^2/4$ and the tree-level amplitude is

$$a_{\text{tree}}(x) = x + \frac{x^2}{M_H^2 - x} \tag{25}$$

Therefore, for $|x| \gg M_H^2$ as in a multi-TeV collider, the tree-level amplitude is governed

([4]) By subtracting quadratic divergences or using dimensional regularization, the logarithmic divergent terms in the ZPE of the various fields are proportional to the fourth power of the mass. Thus, in units of the pure scalar term, one finds $(6M_w^4 + 3M_Z^4)/M_H^4 \lesssim 0.002$ and $12m_t^4/M_H^4 \lesssim 0.05$.

by a contact coupling

$$\lambda_0 = \frac{3M_H^2}{v^2} \tag{26}$$

as in a pure Φ^4 theory. Notice that the tree-level calculation yields λ_0 while, from the Φ^4 effective potential, we found

$$\lambda(v) = \frac{3M_H^2}{\phi_v^2} = \frac{3m_h^2}{v^2} = \frac{m_h^2}{M_H^2}\ \lambda_0 \tag{27}$$

which derives from the assumed "triviality" of the theory. To understand the replacement, let us recall the precise formulation of the Equivalence Theorem given by Bagger and Schmidt [33]. This is a non-perturbative statement in the sense that it holds to all orders in the scalar self-interactions, up to $O(g^2)$ corrections. One then expects that resumming all higher-order graphs in longitudinal WW scattering gives the same result as in a pure Φ^4 if Goldstone $\chi\chi$ diagrams are resummed with the $\beta-$function of Φ^4. This resummation, for $M_H \sim 700$ GeV, means to replace $\lambda_0 \sim 24$ with $\lambda(v) \sim 0.78$. For this reason, no large effect proportional to λ_0 should be visible at the Fermi scale or at the relatively close energies of a multi-TeV collider (where both $\lambda(E)$ and $\lambda^{(p)}(E)$ differ from their common value 0.78 for negligible terms). In this sense, the second resonance will mimic a conventional Higgs particle of mass M_H provided the cutoff independent ratios (M_H^2/v) and $(M_H/v)^2$, in the 3- and 4-order scalar couplings, are re-scaled as follows [34]:

$$\frac{M_H^2}{2v} \to \epsilon_1 \cdot \frac{M_H^2}{2v} \qquad\qquad \frac{M_H^2}{8v^2} \to \epsilon_2 \cdot \frac{M_H^2}{8v^2} \tag{28}$$

with

$$\epsilon_1^2 = \epsilon_2 \equiv \frac{1}{Z_\phi} = \frac{m_h^2}{M_H^2} \tag{29}$$

We can thus predict $\Gamma(H \to WW)$ and $\Gamma(H \to ZZ)$ from their conventional values by replacing the large width $\Gamma^{\rm conv}(H \to WW+ZZ) \sim G_F M_H^3$ with the corresponding value $\Gamma(H \to WW + ZZ) \sim M_H(G_F m_h^2)$ which retains the same phase-space factor M_H but has a coupling re-scaled by the small ratio $m_h^2/M_H^2 \sim 0.032$. Numerically, for $M_H \sim 700$ GeV, from the results of ref. [35], this gives

$$\Gamma(H \to ZZ) \sim \frac{M_H}{700\ \text{GeV}} \cdot \frac{m_h^2}{(700\ \text{GeV})^2}\ 50.1\ \text{GeV} \sim \frac{M_H}{700\ \text{GeV}} \cdot\ 1.6\ \text{GeV} \tag{30}$$

$$\Gamma(H \to WW) \sim \frac{M_H}{700\ \text{GeV}} \cdot \frac{m_h^2}{(700\ \text{GeV})^2}\ 102.6\ \text{GeV} \sim \frac{M_H}{700\ \text{GeV}} \cdot\ 3.3\ \text{GeV} \tag{31}$$

On the other hand, the decays into fermions, gluons, photons...should be unchanged and can be taken from [35] yielding

$$\Gamma(H \to \text{fermions} + \text{gluons} + \text{photons...}) \sim \frac{M_H}{700\ \text{GeV}} \cdot 26\ \text{GeV} \tag{32}$$

Therefore, for $M_H = 670 \div 710$ GeV, one would expect a total width $\Gamma_H \equiv \Gamma(H \to all) = 30 \div 31$ GeV. The above estimate, however, does not account for the new contributions from the decays of the heavier resonance into the lower-mass state at 125 GeV. These include the two-body decay $H \to hh$, the three-body processes $H \to hhh$, $H \to hZZ$, $H \to hW^+W^-$ and the higher-multiplicity final states allowed by phase space. For this reason, the above value $\Gamma_H \sim 30$ GeV should likely represent a lower bound. It is not so simple to evaluate the new contributions to the total decay width because of the $h - H$ overlapping which makes this a non-perturbative problem. Nevertheless, in sect. 4 we will show that some LHC data can be used to constrain experimentally the branching ratio $B(H \to hh) \lesssim 0.12 \div 0.15$ at the 95% C.L. thus leading to $\Gamma_H < 36$ GeV.

Given this theoretical uncertainty, in ref. [13], one considered a test in the "golden" 4-lepton channel that does *not* require the knowledge of the total width and only relies on two assumptions:

a) a resonant 4-lepton production through the chain $H \to ZZ \to 4l$

b) the estimate of $\Gamma(H \to ZZ)$ in eq. (30)

Therefore, by defining $\gamma_H = \Gamma_H / M_H$, we find a fraction

$$B(H \to ZZ) = \frac{\Gamma(H \to ZZ)}{\Gamma_H} \sim \frac{1}{\gamma_H} \cdot \frac{50.1}{700} \cdot \frac{m_h^2}{(700 \text{ GeV})^2} \tag{33}$$

that will be replaced in the cross section approximated by on-shell branching ratios

$$\sigma_R(pp \to H \to 4l) \sim \sigma(pp \to H) \cdot B(H \to ZZ) \cdot 4B^2(Z \to l^+l^-) \tag{34}$$

This should be a good approximation for a relatively narrow resonance so that one predicts a particular correlation

$$\gamma_H \cdot \sigma_R(pp \to H \to 4l) \sim \sigma(pp \to H) \cdot \frac{50.1}{700} \cdot \frac{m_h^2}{(700 \text{ GeV})^2} \cdot 4B^2(Z \to l^+l^-) \tag{35}$$

which can be compared with the LHC data.

Since $4B^2(Z \to l^+l^-) \sim 0.0045$, to check our prediction, the last ingredient is the total production cross section $\sigma(pp \to H)$ which, in our case, will mainly proceed through the gluon-gluon Fusion (ggF) process. In fact, the other production through Vector-Boson Fusion (VBF) plays no role here, once the large coupling to longitudinal W's and Z's is suppressed by the small coefficient $m_h^2/M_H^2 \sim 0.032$. As a consequence the traditional large VBF cross section $\sigma^{\text{VBF}}(pp \to H) \sim 300$ fb is reduced to about 10 fb and can be safely neglected in comparison with the pure ggF contributions $\text{O}(10^3)$ fb. Indeed, for 13 TeV pp collisions and and with a typical $\pm 15\%$ uncertainty (due to the parton distributions, to the choice of μ in $\alpha_s(\mu)$ and to other effects), we will adopt the value [36] $\sigma^{\text{ggF}}(pp \to H) = 1090(170)$ fb which also accounts for the range $M_H = 660 \div 700$ GeV.

In conclusion, for $m_h = 125$ GeV, one obtains a prediction which, for not too large γ_H where eq. (34) looses validity, is formally insensitive to the value of Γ_H and can be directly compared with the 4-lepton data

$$[\gamma_H \cdot \sigma_R(pp \to H \to 4l)]^{\text{theor}} \sim (0.011 \pm 0.002) \text{ fb} \tag{36}$$

4. – Some experimental signals from LHC

To test our definite prediction $(M_H)^{\rm Theor} = 690 \pm 10(\text{stat}) \pm 20(\text{sys})$ GeV, one should look for deviations from the background nearby. This means that local deviations from background should not be downgraded by the so called "look elsewhere" effect. At the same time, given the present energy and luminosity of LHC, the second resonance, if there, is too heavy to be seen unambiguously in all possible channels. In this sense, one should remember the h(125) discovery which, at the beginning, was giving no signals in the predominant $b\bar{b}$ and $\tau^+\tau^-$ decay channels.

After this premise, given the expected large branching ratio $B(H \to t\bar{t}) = (75 \div 80)\%$, the most natural place to look for the new resonance would be in the $t\bar{t}$ channel. However, in the relevant region of invariant mass $m(t\bar{t}) = 620 \div 820$ GeV, CMS measurements [37] give a background cross section $\sigma(pp \to t\bar{t}) = 107 \pm 7.6$ pb which is about 100 times larger than the expected signal $\sigma(pp \to H \to t\bar{t}) \lesssim 1$ pb ([5]). For this reason, in refs. [13-16] the phenomenological analysis was focused on available channels with relatively smaller background, namely:

i) ATLAS ggF-like 4-lepton events
ii) ATLAS high-mass inclusive $\gamma\gamma$ events
iii) ATLAS and CMS $(b\bar{b} + \gamma\gamma)$ events
iv) CMS $\gamma\gamma$ events exclusively produced in pp double-diffractive scattering

4˙1. *The ATLAS ggF-like 4-lepton events.* – As a first sample, we started from the ATLAS charged 4-lepton channel [40, 41] by considering those events that, for their characteristics, can be interpreted as being produced through the ggF mechanism. For these 4-lepton data, the ATLAS experiment has performed a sophisticated analysis where the ggF events, depending on the degree of contamination with the background, are divided into four mutually exclusive categories: ggF-high-4μ, ggF-high- 2e2μ, ggF-high-4e, ggF-low. The only sample which is homogeneous from the point of view of the selection and has a sufficient statistics is the ggF-low category whose number of events are reported in table II together with the background estimated by ATLAS, see ref. [41]. To avoid spurious fluctuations which may be due to migration of events between adjacent bins, we have followed the same criterion adopted in fig. 5 of the other ATLAS paper ref. [42] where events were grouped in larger bins of 60 or even 80 GeV ([6])

From this table II, one gets the same impression as from fig. 5 of ref. [42] in the same energy region. Namely, there is a $+2.5\,\sigma$ excess over the background, in the bin centered around 680 GeV, which is followed by a $-3\,\sigma$ defect in the bin centered around 740 GeV. The simplest explanation for these two simultaneous features would be the existence of a resonance of mass $M_H \sim 700$ GeV which, above the Breit-Wigner peak, produces the characteristic negative interference pattern proportional to $(M_H^2 - s)$.

([5]) Interestingly, the process $pp \to t\bar{t}t\bar{t}$ has now been observed by ATLAS [38] and CMS [39]. Both experiments find cross sections which are somewhat larger than the SM prediction $\sigma_B(pp \to t\bar{t}t\bar{t}) = 12.0 \pm 2.4$ fb. Namely, $22.5^{+6.6}_{-5.5}$ fb (ATLAS) and $17.7^{+4.4}_{-4.0}$ fb (CMS). This excess could indicate the process $pp \to H$ with the H resonance decaying into a virtual pair of $h = h(125)$ followed by two $h \to t\bar{t}$ decays. Therefore, it would be interesting to determine the invariant mass distribution of the $t\bar{t}t\bar{t}$ system.

([6]) This is because in the region of invariant mass around 700 GeV the energy resolution varies considerably from about 12 GeV for $4e$ events, to 19 GeV for $2e2\mu$ up to 24 GeV for 4μ.

TABLE II. – *For luminosity 139 fb^{-1}, we report the observed ATLAS ggF-low events and the corresponding estimated background* [41] *in the range of invariant mass $M_{4l} = E = 530 \div 830$ GeV. To avoid spurious fluctuations, due to migration of events between neighbouring bins, we have followed the same criterion as in fig. 5 of ref.* [42] *by grouping the data into larger bins of 60 GeV, centered at 560, 620, 680, 740 and 800 GeV. These correspond to the 10 bins of 30 GeV, centered respectively at: 545(15)÷ 575(15) GeV, 605(15)÷ 635(15) GeV, 665(15) ÷ 695(15), 725(15)÷755(15) GeV and 785(15)÷ 815(15) GeV, see ref.* [41]*. In this energy range, the uncertainties in the background are below* 5% *and will be neglected.*

E[GeV]	$N_{EXP}(E)$	$N_B(E)$	$N_{EXP}(E) - N_B(E)$
560(30)	38±6.16	32.0	6.00 ± 6.16
620(30)	25±5.00	20.0	5.00 ± 5.00
680(30)	26±5.10	13.04	12.96 ± 5.10
740(30)	3±1.73	8.71	-5.71 ± 1.73
800(30)	7±2.64	5.97	1.03 ± 2.64

To describe the data in table II, one adopted the model cross section of ref. [12, 13]

$$\sigma_T = \sigma_B + \frac{2(M_H^2 - s)\,\Gamma_H M_H}{(s - M_H^2)^2 + (\Gamma_H M_H)^2}\,\sqrt{\sigma_B \sigma_R} + \frac{(\Gamma_H M_H)^2}{(s - M_H^2)^2 + (\Gamma_H M_H)^2}\,\sigma_R \tag{37}$$

where, together with the mass M_H and total width Γ_H of the resonance, one introduces a background cross section $\sigma_B = \sigma_B(E)$ and the resonating peak cross section σ_R.

An accurate description of the ATLAS background can be obtained in terms of a power law $N_B(E) \sim A \cdot (710\ \text{GeV}/E)^\nu$ with $A \sim 10.55$ and $\nu \sim 4.72$. Then, by simple redefinitions, the theoretical number of events can be expressed as

$$N_{TH}(E) = N_B(E) + \frac{P^2 + 2P \cdot x(E) \cdot \sqrt{N_B(E)}}{\gamma_H^2 + x^2(E)} \tag{38}$$

TABLE III. – *We report the observed ATLAS ggF-low events and our theoretical prediction eq. (38) for $M_H = 706$ GeV, $\gamma_H = 0.041$, $P = 0.14$.*

E[GeV]	$N_{EXP}(E)$	$N_{TH}(E)$	χ^2
560(30)	38±6.16	36.72	0.04
620(30)	25±5	25.66	0.02
680(30)	26±5.10	26.32	0.00
740(30)	3±1.73	3.23	0.02
800(30)	7±2.64	3.87	1.40

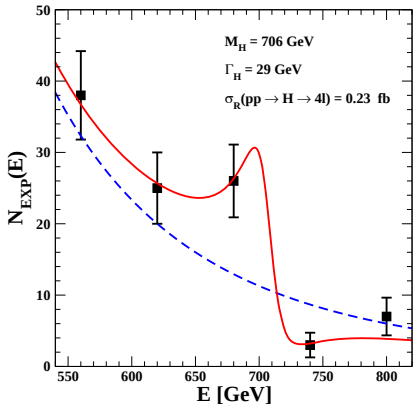

Fig. 2. – *The values* $\mathrm{N_{EXP}(E)}$ *in table II vs. the corresponding* $\mathrm{N_{TH}(E)}$ *eq. (38) (the red continuous line). The resonance parameters are* $M_H = 706$ *GeV,* $\gamma_H = 0.041$*,* $\sigma_R = 0.23$ *fb and the ATLAS background is approximated as* $N_B(E) = A \cdot (710\ \mathrm{GeV}/E)^{\nu}$ *with* $A = 10.55$ *and* $\nu = 4.72$*.*

where $x(E) = (M_H^2 - E^2)/M_H^2$, $N_R = \sigma_R \cdot \mathcal{A} \cdot 139\ \mathrm{fb}^{-1}$ denotes the extra events at the resonance peak for an acceptance $\mathcal{A}$ and finally $P \equiv \gamma_H \sqrt{N_R}$.

As for the acceptance, one adopted a value $\mathcal{A} \sim 0.38$ by averaging the two extremes, 0.30 and 0.46, for the ggF-like category of events [40]. As a consequence, the resonance parameters are affected by some uncertainty. Nevertheless, to have a first check of our picture, we fitted with eq. (38) the experimental number of events in table II. The results were: $M_H = 706(25)$ GeV, $\gamma_H = 0.041 \pm 0.029$ (corresponding to a total width $\Gamma_H = 29 \pm 20$ GeV) and $P = 0.14 \pm 0.07$. From these we obtain $N_R \sim 12$ and $\sigma_R \sim 0.23$ fb with very large errors. Our theoretical values are shown in table III and a graphical comparison in fig. 2.

The quality of the fit is good but, with the exception of the mass, errors are large and a test of our picture is not so stringent. Still, with the partial width of sect. 3,

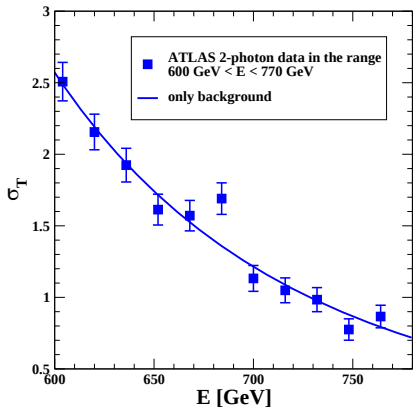

Fig. 3. – *The fit with eq. (37) and* $\sigma_R = 0$ *to the data in table IV, transformed into cross-sections in fb. The chi-square value is* $\chi^2 = 14$ *and the background parameters* $A = 1.35$ *fb and* $\nu = 4.87$*.*

TABLE IV. – *The ATLAS number $N = N(\gamma\gamma)$ of events, in bins of 16 GeV and for luminosity 139 fb^{-1}, for the range of invariant mass $\mu = \mu(\gamma\gamma) = 600 \div 770$ GeV. These values were extracted from fig. 3 of* [43] *because the relevant numbers are not reported in the companion HEPData file. In our fits we assumed as statistical errors the square root of the counts as for a Poisson distribution.*

μ	604	620	636	652	668	684	700	716	732	748	764
N	349	300	267	224	218	235	157	146	137	108	120

$\Gamma(H \to ZZ) \sim 1.6$ GeV, and fixing Γ_H to its central value of 29 GeV, we find a branching ratio $B(H \to ZZ) \sim 0.055$ which, for the central value $\sigma^{\rm ggF}(pp \to H) \sim 923$ fb of ref. [36] at $M_H = 700$ GeV, would imply a theoretical peak cross section $(\sigma_R)^{\rm theor} = 923 \cdot 0.055 \cdot 0.0045 \sim 0.23$ fb which coincides with the central value from our fit. Also from the central values $\langle\sigma_R\rangle = 0.23$ fb and $\langle\gamma_H\rangle = 0.041$, we find $\langle\sigma_R\rangle \cdot \langle\gamma_H\rangle \sim 0.0093$ fb, consistently with eq. (36).

4˙2. *The ATLAS high-mass $\gamma\gamma$ events.* – Searching for further signals, in refs. [15,16] one considered the invariant mass distribution of the inclusive diphoton production as measured by ATLAS [43] in the range of invariant mass $600 \div 770$ GeV. The relevant entries in table IV were extracted from fig. 3 of [43] because the numerical values are not reported in the companion HEPData file. By parameterizing the background with a power-law form $\sigma_B(E) \sim A \cdot (685\ {\rm GeV}/E)^\nu$ to the data in table 3 gives a good description of all data points, except the sizeable excess at 684 GeV (estimated by ATLAS to have a local significance of more than 3-sigma) see fig. 3.

This isolated discrepancy illustrates how a (hypothetical) new resonance might remain hidden behind the large background almost everywhere, the main signal being just a modest interference effect. For this reason, with the exception of the mass $M_H = 696(13)$ GeV, the total decay width is determined very poorly. Namely $\Gamma_H = 15^{+30}_{-12}$ GeV, in agreement with the other loose determination $\Gamma_H = 29(20)$ GeV from the 4-lepton data. In fig. 4 we report three fits with the full eq. (37) for $\Gamma_H = 15$, 25 and 35 GeV. In conclusion, the localized 3 sigma excess at 684 GeV admits two different interpretations:

a) a statistical fluctuation above a pure background, see fig. 3
b) the signal of a heavy, relatively narrow resonance, see fig. 4

4˙3. *ATLAS and CMS $(b\bar{b} + \gamma\gamma)$ events.* – The ATLAS and CMS Collaboration have also considered the search for new resonances decaying, through two intermediate $h(125)$ scalars, into the peculiar final state made by a $b\bar{b}$ quark pair and a $\gamma\gamma$ pair. In particular, in [44] one has been considering the cross section for the full process

$$\sigma({\rm full}) = \sigma(pp \to X \to hh \to b\bar{b} + \gamma\gamma) \tag{39}$$

For a spin-zero resonance, the 95% upper limit $\sigma({\rm full}) < 0.16$ fb, for invariant mass of 600 GeV, was found to increase by about a factor of two, up to $\sigma({\rm full}) < 0.30$ fb in a plateau $650 \div 700$ GeV, and then to decrease for larger energies see fig. 5. The local statistical significance is modest, about 1.6-sigma, but the relevant mass region $M_X \sim 675(25)$ GeV is precise and agrees well with our prediction. Interestingly, if the cross

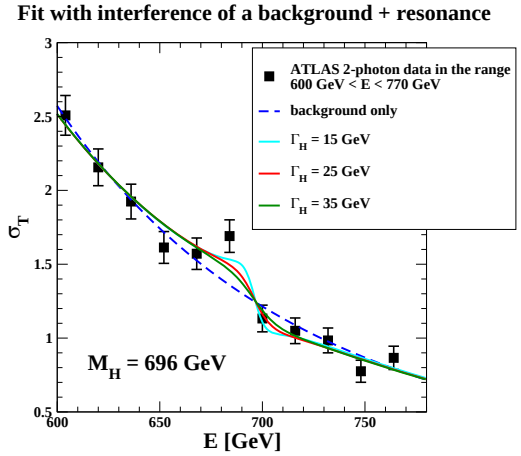

Fig. 4. – *Three fits with eq. (37) to the data in table IV, transformed into cross-sections in fb. The* χ^2-*values are 7.5, 8.8, 10.2, respectively for* $\Gamma_H = 15,\ 25$ *and* 35 *GeV.*

section is approximated as

$$\sigma(\text{full}) \sim \sigma(pp \to H) \cdot B(H \to hh) \cdot 2 \cdot B(h \to b\bar{b}) B(h \to \gamma\gamma) \tag{40}$$

the CMS 95% upper bound $\sigma(\text{full}) < 0.30$ fb, for $\sigma(pp \to H) \sim 1$ pb, becomes an upper bound $B(H \to hh) < 0.12$. In view of the mentioned non-perturbative nature of the decay process $H \to hh$ this represents a precious indication.

The analogous ATLAS plot is reported in fig. 6 (which is the same fig. 15 of the ATLAS paper [45]). Again, one finds a modest 1.2-sigma excess in the plateau 650(25) GeV which is followed immediately by a 1.4-sigma defect which could be indicative of a negative above-peak $(M_H^2 - s)$ interference effect of the same type found in the ATLAS 4-lepton data. From the observed value $\sigma(pp \to H \to hh) < 150$ fb, this gives $B(H \to hh) < 0.15$, consistent with the CMS determination. Since the 3-body decays $H \to hhh$, $H \to hW^+W^-$, $H \to hZZ$ should give a modest contribution to the total width, from the estimates of sect. 3, we would then deduce $\Gamma_H < 36$ GeV.

4˙4. *CMS* $\gamma\gamma$ *events exclusively produced in pp double-diffractive scattering.* – Finally, the CMS and TOTEM Collaborations have been searching for high-mass photon pairs exclusively produced in pp double-diffractive scattering, *i.e.*, when both final protons have large x_F. For our scopes, the relevant information is contained in fig. 7 taken from [46]. In the range of invariant mass 650(40) GeV, and for a statistics of 102.7 fb^{-1} the observed number of $\gamma\gamma$ events was $N_{\text{OBS}} \sim 76(9)$ to be compared with an estimated background $N_{\text{BKG}} \sim 40(6)$ that is quoted to be the best estimate by the experiment, with a relatively small uncertainty. In the most conservative case, this is a local 3-sigma effect and is the only statistically significant excess in the plot.

4˙5. *Experimental summary.* – Let us summarize the previous analysis of LHC data:

i) after observing the +2.5 sigma excess at 680(30) GeV and the simultaneous −3.3 sigma defect at 740(30) GeV in the ATLAS ggF-like 4-lepton events, a fit to this data was performed in [15, 16]. The resulting mass value was $M_H = 706(25)$ GeV

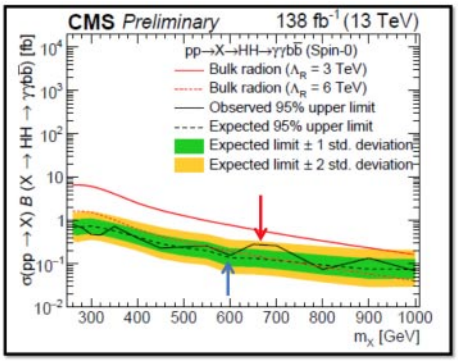

Fig. 5. – *Expected and observed 95% upper limit for the cross section* $\sigma(pp \to X \to h(125)h(125) \to b\bar{b} + \gamma\gamma)$ *observed by the CMS Collaboration* [44].

ii) after observing the +3 sigma effect at 684(16) GeV in the inclusive ATLAS $\gamma\gamma$ events, a fit to this data was performed in [15,16]. The resulting mass was $M_H = 696(13)$ GeV

Furthermore, one should note

iii) the overall +2 sigma effect in the ($b\bar{b}$+$\gamma\gamma$) channel which is obtained by combining the excess of events observed by ATLAS at 650(25) GeV and the corresponding excess observed by CMS at 675(25) GeV

iv) the +3 sigma excess at 650(40) GeV in the distribution of CMS-TOTEM $\gamma\gamma$ events exclusively produced in *pp* double-diffractive scattering

Since the above determinations i)-iv) are well aligned within the uncertainties, one can try to combine the mass values by obtaining $(M_H)^{\rm comb} \sim 685(10)$ GeV in very good agreement with our prediction $(M_H)^{\rm Theor} = 690 \pm 10$ (stat) $\pm$ 20(sys) GeV. I emphasize again that, when comparing with a definite prediction, one should look for deviations from the background nearby so that local significance is not downgraded by the so called "look elsewhere" effect. Thus, in view of the small correlation of the above determinations, one could also argue that the cumulative statistical evidence for a new resonance around 700 GeV is close to (if not above) the traditional 5-sigma level. Anyway, the present situation is unstable and could soon be resolved with two still missing sets of RUN2 data, namely

a) the full CMS charged 4-lepton events

b) the full CMS inclusive high-mass $\gamma\gamma$ events

By adding these two crucial sets of data, the present, non-trivial statistical significance could become an important new discovery.

5. – Summary and conclusions

The perturbative effective potential of the Standard Model, say $V^{(\rm p)}(\phi)$, exhibits a second minimum $v_{\rm true} = 10^{26} \div 10^{31}$ GeV, well beyond the Planck mass, which is much deeper than the electroweak vacuum at $v \sim 246$ GeV, *i.e.*, $V^{(\rm p)}(v_{\rm true}) = -(10^{100} \div 10^{120})$ $(\rm GeV)^4$ *vs.* $V^{(\rm p)}(v) \sim -10^8$ $(\rm GeV)^4$. Since it is uncertain that gravitational effects can become so strong to stabilize the potential, one has accepted the metastability scenario in a cosmological perspective. This perspective is needed to explain why the theory remains trapped into the tiny electroweak minimum but requires to control the properties of matter in the extreme conditions of the early Universe. As an alternative, we have reviewed the completely different idea of an effective potential which, as at beginning

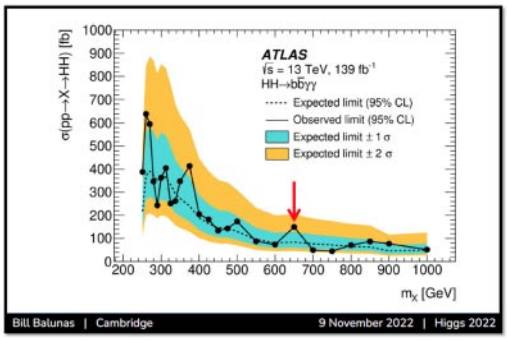

Fig. 6. – *Expected and observed 95% upper limit for the cross section* $\sigma(pp \to X \to h(125)h(125))$ *extracted by the ATLAS Collaboration from the final state* $(b\bar{b} + \gamma\gamma)$. *The figure is taken from the talk given by Bill Balunas at Higgs 2022 and is the same fig. 15 of the ATLAS paper* [45].

of the Standard Model, is restricted to the pure Φ^4 sector but is consistent with the now existing analytical and numerical studies. In this approach, where the absolute minimum is at $v \sim 246$ GeV, the effective potential, beside the mass $m_h = 125$ GeV, defined by its quadratic shape at the minimum, should exhibit a second much larger mass scale M_H associated with the zero-point energy which determines the potential depth. By combining analytical and numerical indications, one arrives to the estimate $(M_H)^{\text{theor}} = 690 \pm 10$ (stat) ± 20 (sys) GeV. With such a large mass, the ZPE of all known gauge and fermion fields would represent a small radiative correction. Thus, by restricting to a region around the Fermi scale, say a few TeV, the different evolution of $\lambda^{(\text{p})}(\phi)$ and of $\lambda(\phi)$ at asymptotically large ϕ should remain unobservable and the check is demanded to the experimental observation of the second resonance.

In spite of its large mass, however, the second resonance should couple to longitudinal W's with the same typical strength as the low-mass state at 125 GeV and thus represent a relatively narrow resonance of width $\Gamma_H = 30 \div 36$ GeV, mainly produced at LHC by gluon-gluon fusion. For this reason, it is remarkable that in the LHC data one can find indications for a new resonance in the expected mass range with a statistical significance that is far from negligible and could become an important new discovery by just adding two missing samples of RUN2 data.

Before concluding, we will briefly discuss the possible implications of this two-mass structure for radiative corrections. A propagator structure as in eq. (15) suggests that, for very large Λ, there should be two vastly different mass-shell regions in Minkowski space, as when the spectral density has not the standard single-peak structure. This brings in touch with the work of van der Bij [47] where a propagator form which resembles eq. (15) was considered. On the basis of other arguments, quite unrelated to the effective potential, he speculated that the physical Higgs boson could be a mixture of two states with a spectral density approximated by two $\delta-$functions and propagator $(-1 \leq \eta \leq 1)$

$$G(p) \sim \frac{1-\eta}{2}\frac{1}{p^2+m_h^2} + \frac{1+\eta}{2}\frac{1}{p^2+M_H^2} \tag{41}$$

This structure could be used in radiative corrections, for instance in the $\rho-$parameter. For masses below 1 TeV, where the 2-loop correction is completely negligible, one can restrict to the one-loop level, where the two branches eq. (41) do not mix. Then, the net effect would be to replace in the main logarithmic term an effective mass $m_{\text{eff}} \sim$

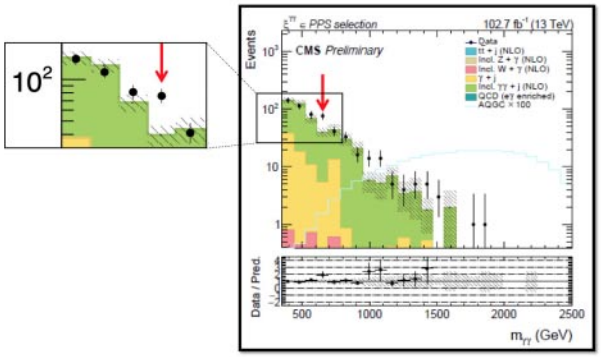

Fig. 7. – *The number of $\gamma\gamma$ events exclusively produced in pp double-diffractive scattering as reported in* [46]. *In the range 650(40) GeV, the observed number was $N_{\rm OBS} \sim 76(9)$ to be compared with an estimated background $N_{\rm BKG} \sim 40(6)$.*

$\sqrt{m_h M_H}\ (M_H/m_h)^{\eta/2}$. In our case, the spectral function has a crossover region and would not be the simple sum of two $\delta-$functions. Nevertheless, one could still consider this idea and explore how well the mass parameter $m_{\rm eff}$, obtained indirectly from radiative corrections agrees with the $m_h = 125$ GeV, measured directly at LHC. Here we just report the two extreme indications from the PDG review [17]. Namely, from the experimental set ($A_{\rm LR}$, M_Z, Γ_Z, m_t), one finds the pair [$m_{\rm eff} = 38^{+30}_{-21}$ GeV, $\alpha_s(M_z) = 0.1182(47)$]. While, from the set ($A_{\rm FB}(b,c)$, M_Z, Γ_Z, m_t), the other pair [$m_{\rm eff} = 348^{+187}_{-124}$ GeV, $\alpha_s(M_z) = 0.1278(50)$].

These two extreme cases show that, at this level of precision, one should estimate the uncertainty due to strong interactions. This enters through the contribution of hadronic vacuum polarization to $\Delta\alpha(M_z)$, but also more directly through the value of $\alpha_s(M_z)$. More precisely, in the two examples considered above, this latter uncertainty enters through $r_s(M_z)$, the strong-interaction correction to the quark-parton model in $\sigma(e^+e^- \to hadrons)$ at center of mass energy $Q = M_z$. Since, for a given m_t, $r_s(M_z)$ and $m_{\rm eff}$ are positively correlated in the hadronic W and Z widths, in a global fit, through the W and Z widths and the LEP1 peak cross sections, the uncertainty in $r_s(M_z)$ will propagate and affect all quantities, even the pure leptonic widths and asymmetries.

This uncertainty should not be underestimated because, in the ($e^+e^- \to hadrons$) data from PETRA, PEP, TRISTAN there is a sizeable excess with respect to the perturbative QCD prediction [48]. By including all data up to LEP2, the excess can be estimated at the 4-sigma level [49]. Therefore, since a small coupling does not guarantee, by itself, a good convergence of the perturbative expansion, one should seriously consider that, even at large center of mass energies, the experimental quantity $r^{\rm EXP}(Q)$ obtained from the data can sizeably differ from its theoretical prediction $r_s^{\rm TH}(Q) = 1+\alpha_s(Q)/\pi+...$ computed from the first few terms. If translated into the QCD correction, the observed excess corresponds to replacing the higher range of values $\alpha_s(M_z) \gtrsim 0.128$ in $r^{\rm TH}(M_z)$ and, if used to evaluate the EW corrections, would increase considerably the value of $m_{\rm eff}$ obtained from many experimental quantities. As such, the present view, that the Higgs mass parameter extracted indirectly from radiative corrections agrees perfectly with the $m_h = 125$ GeV measured directly at LHC, is not free of ambiguities.

* * *

We thank Giorgio Bellettini, Giorgio Chiarelli, Mario Greco and Gino Isidori for their invitation to contribute to the Conference.

REFERENCES

[1] ATLAS Collaboration (Aad G. *et al.*), *Phys. Lett. B*, **716** (2012) 1.
[2] CMS Collaboration (Chatrchyan S. *et al.*), *Phys. Lett. B*, **716** (2012) 30.
[3] Branchina V. and Messina E., *Phys. Rev. Lett.*, **111** (2013) 241801.
[4] Gabrielli E., Heikinheimo M., Kannike K., Racioppi A, Raidal M. and Spethmann C., *Phys. Rev. D*, **89** (2014) 015017.
[5] Degrassi G., Di Vita S., Miró J. E., Espinosa J. R., Giudice G. F., Isidori G. and Strumia A., *JHEP*, **08** (2012) 098.
[6] Salvio A., Strumia A., Tetradis N. and Urbano A., *JHEP*, **09** (2016) 054.
[7] Branchina V., Messina E. and Zappalà D., *Impact of Gravity on Vacuum Stability*, arXiv:1601.06963v2 [hep-ph].
[8] Markkanen T., Rajantie A. and Stopyra S., *Front. Astron. Space Sci.*, **5** (2018) 00040.
[9] Espinosa J. R., Giudice G. and Riotto A., *JCAP*, **05** (2008) 002.
[10] Consoli M. and Cosmai L., *Int. J. Mod. Phys. A*, **35** (2020) 2050103, arXiv:hep-ph/2006.15378.
[11] Consoli M. and Cosmai L., *Symmetry*, **12** (2020) 2037.
[12] Consoli M., *Acta Phys. Pol. B*, **52** (2021) 763, arXiv:2106.06543 [hep-ph].
[13] Consoli M. and Cosmai L., *Int. J. Mod. Phys. A*, **37** (2022) 2250091, arXiv:2111.08962 v3 [hep-ph].
[14] Consoli M., Cosmai L. and Fabbri F., *PoS*, **ICHEP2022** (2022) 204.
[15] Consoli M., Cosmai L. and Fabbri F., arXiv:2208.00920v2 [hep-ph], revised version December 2022.
[16] Consoli M., Cosmai L. and Fabbri F., *Universe*, **9** (2023), MDPI Special Issue, "BSM and Higgs Physics".
[17] Particle Data Group (Tanabashi M. *et al.*), *Phys. Rev. D*, **98** (2018) 030001.
[18] Coleman S. R. and Weinberg E. J., *Phys. Rev. D*, **7** (1973) 1888.
[19] Lundow P. H. and Markström K., *Phys. Rev. E*, **80** (2009) 031104.
[20] Lundow P. H. and Markström K., *Nucl. Phys. B*, **845** (2011) 120.
[21] Akiyama S. *et al.*, *Phys. Rev. D*, **100** (2019) 054510.
[22] Lundow P. H. and Markström K., *Nucl. Phys. B*, **993** (2023) 116256.
[23] Gliozzi F., *Nucl. Phys. B Proc. Suppl.*, **63** (1998) 634, arXiv:hep-lat/9709062.
[24] Consoli M. and Stevenson P. M., *Int. J. Mod. Phys. A*, **15** (2000) 133.
[25] Feinberg G. and Sucher J., *Phys. Rev.*, **166** (1968) 1638.
[26] Feinberg G., Sucher J. and Au C. K., *Phys. Rep.*, **180** (1989) 83.
[27] Stevenson P. M., *Mod. Phys. Lett. A*, **24** (2009) 261, arXiv:0806.3690 [hep-ph].
[28] 't Hooft G., *Search of the Ultimate Building Blocks* (Cambridge University Press) 1997, p.70.
[29] Stevenson P. M., *Phys. Rev. D*, **32** (1985) 1389.
[30] Stevenson P. M., *Nucl. Phys. B*, **729** (2005) 542.
[31] Lang C. B., *Computer Stochastics in Scalar Quantum Field Theory, Proceedings of NATO Advanced Study Institute on Stochastic Analysis and Applications in Physics* (Springer Science+Business Media) 1993, p. 133, arXiv:hep-lat/9312004.
[32] Veltman M. J. G. and Yndurain F. J., *Nucl. Phys. B*, **325** (1989) 1.
[33] Bagger J. and Schmidt C., *Phys. Rev. D*, **41** (1990) 264.
[34] Castorina P., Consoli M. and Zappalà D., *J. Phys. G*, **35** (2008) 075010.
[35] *BSM Higgs production cross sections at* $\sqrt{(s)}$*=13 TeV* (update in CERN Report4 2016) `https://twiki.cern.ch/twiki/bin/view/LHCPhysics/CERNYellowReportPageBSMAt13TeV`.

[36] https://twiki.cern.ch/twiki/bin/view/LHCPhysics/CERNYellowReportPageAt13TeV.
[37] CMS Collaboration, *JHEP*, **02** (2019) 149, arXiv:1811.06625v2 [hep-ex].
[38] ATLAS Collaboration, *Observation of four-top-quark production in the multilepton final state with the ATLAS detector*, arXiv:2303.15061v2 [hep-ex] (29 June 2023).
[39] CMS Collaboration, *Observation of four top quark production in proton-proton collisions at* $\sqrt{s} = 13$ *TeV*, arXiv:2305.13439v1 [hep-ex] (22 May 2023).
[40] ATLAS Collaboration, *Eur. Phys. J. C*, **81** (2021) 332, arXiv:2009.14791[hep-ex].
[41] https://www.hepdata.net/record/ins1820316.
[42] ATLAS Collaboration, *JHEP*, **07** (2021) 005, arXiv:2103.01918v1 [hep-ex].
[43] ATLAS Collaboration, *Phys. Lett. B*, **822** (2021) 136651.
[44] CMS Collaboration, *Search for a new resonance decaying to two scalars in the final state with two b-quarks and two photons in pp collisions at* $\sqrt{s} = 13$ *TeV*, CMS PAS HIG-21-011.
[45] ATLAS Collaboration, *Phys. Rev. D*, **106** (2022) 052001.
[46] CMS and TOTEM Collaborations, *Search for high-mass exclusive diphoton production with tagged protons*, CMS PAS EXO-21-007 and TOTEM NOTE 22-005.
[47] van der Bij J. J., *Acta Phys. Pol. B*, **11** (2018) 397.
[48] Branchina V., Consoli M., Fiore R. and Zappalà D., *Phys. Rev. D*, **46** (1992) 75.
[49] Schmitt M., *Apparent Excess in* $e^+e^- \to hadrons$, arXiv:hep-ex/0401034v2.